Pergamon

Bioorganic & Medicinal Chemistry Letters 12 (2002) 61–64

BIOORGANIC & MEDICINAL CHEMISTRY LETTERS

3-D QSAR Studies on New Dibenzyltin(IV) Anticancer Agents by Comparative Molecular Field Analysis (CoMFA)

Purnima M. Samuel,[a] Dick de Vos,[b] D. Raveendra,[c] J. A. R. P. Sarma[c,*] and Sujit Roy[d,*]

[a]*Metallo-Organic Laboratory, Indian Institute of Chemical Technology, Hyderabad 500007, India*
[b]*Medical Department, Pharmachemie BV, PO Box 552, 2003 RN Haarlem, The Netherlands*
[c]*Molecular Modeling Group, Organic Division-I, Indian Institute of Chemical Technology, Hyderabad 500007, India*
[d]*Organometallics & Catalysis Laboratory, Chemistry Department, Indian Institute of Technology, Kharagpur 721302, India*

Received 3 August 2001; accepted 8 October 2001

Abstract—Dibenzyltin(IV)dichloride and dibenzyltin(IV)diisothiocyanate derivatives with N,S-donor ligands show significant cytotoxic activities against human cancer cell lines, and are well compared to analogous dialkyltin(IV) derivatives. CoMFA models were generated for the first time for these organotin derivatives using the cytotoxic activities (against two human tumor cell lines, MCF-7, a mammary carcinoma and WiDr, a colon carcinoma) of 21 complexes. High r^2 and r^2_{cv} values for both CoMFA models indicate good predictive power for the models. © 2001 Published by Elsevier Science Ltd.

Following the path-breaking success of cisplatin and carboplatin as effective anticancer drugs, attempts have been made to design other transition and non-transition metal complexes as cytotoxic agents.[1] In the past two decades, a large number of organotin(IV) complexes have been developed chiefly by Crowe et al. and Gielen et al., with promising in vitro and in vivo antitumor activities.[2–4] Such compounds are either modeled as analogues of cisplatin, or have novel tetracoordinated structures. In particular, organotin(IV) complexes of the formula $R_2SnX_2.L_n$, where R represents Me, Et, Pr, Bu, c-hexyl, and Ph groups; X represents a halogen; and L represents mono- ($n=2$) or bidentate ($n=1$) ligands having N or O donor atoms, were shown to display significant antitumor activity against P388 lymphocytic leukemia in mice.[5,6] The above studies have further revealed that: (a) diethyl and/or diphenyltin complexes posses higher activities; (b) there is no real link between the Lewis acidity of the parent organotin halide and the P-388 inhibition activity; (c) the mode of DNA-binding for these complexes must have a different mechanism than that of cisplatin; (d) a pre-dissociation of the bidentate ligand may be the rate determining step in vivo; and (e) several complexes show poor activity against human cancer cell lines. In short, a structure versus tumor inhibition activity relationship in this particular group of complexes is yet to emerge.

In continuation of our studies[7] on the chemical and biological role of organotin, we present herein cytotoxicity studies of a series of new dibenzyltin(IV) compounds of general formula $Bn_2SnX_2L_n$ (where Bn = benzyl, X = halide, pseudohalide, L = mono ($n=2$) or bidentate ($n=1$) N,S-donor ligands). The organotin complexes showed promising in vitro antitumor activities against several human cancer cell lines. Furthermore, a QSAR analyses have been performed from the cytotoxic activity against two human tumor cell lines, MCF-7 (a mammary carcinoma) and WiDr (colon carcinoma). The complexes that were included in such analyses were part of those reported here as well as found in the literature.[8] The new organotin derivatives were synthesized from dibenzyltindichloride, and dibenzyltindiisothiocyanate by complexing with N,S-donor ligands in 1:2 (monodentate) or 1:1 (bidentate) stoichiometry. They are fully characterized by ^1H, ^{13}C, ^{119}Sn NMR, IR, X-ray crystallography and satisfactory elemental analysis.

In Vitro Cytotoxicity and In Vivo Mammalian Toxicity

The dibenzyltin(IV) complexes (Scheme 1) have been subjected to in vitro antitumor screening against human

*Corresponding author. Tel.: +91-3222-93338; fax: +91-3222-755303; e-mail: sroy@chem.iitkgp.ernet.in

0960-894X/02/$ - see front matter © 2001 Published by Elsevier Science Ltd.
PII: S0960-894X(01)00684-9

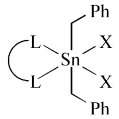

Code	L	X
1	Pyridine	Cl
2	Imidazole	Cl
3	Thiophene	Cl
4	Indole	Cl
5	Indole	NCS
6	Phenanthroline	Cl
7	Bipyridine	Cl
8	Bipyridine	NCS

Scheme 1.

cancer cell lines. Tests were conducted on six cell lines using SRB-assay technique, and on 60-cell lines panel under NCI developmental therapeutics program.[9] The data (Table 1) strongly suggest the superior in vitro cytotoxic activity of a number of dibenzyltin(IV) complexes over cisplatin and carboplatin. Qualitatively, the cytotoxicity is found to be cell line as well as ligand specific. Thus, for chloride complexes the overall toxicity against renal, ovarian, and breast cancer cell lines are higher as compared to melanoma, colon, and non-small cell lung cancer. No activity whatsoever was found for leukemia cell line. It is further interesting to note that the dibenzyltin(IV) complexes offer excellent selectivity against all the six sub-panels of renal cancer cell lines. This is particularly encouraging since the platinum compounds exhibit poor activities against renal cancer.

With respect to ligand effects, thiophene complex **3** is most cytotoxic. Indole **4**, phenanthroline **6**, and bipyridyl **7** complexes show similar toxicity, while pyridine complex **1** is inactive. Limited data prevents a comparison between chloro versus isothiocyanate complexes. Influence of dissociating behavior of Sn–Cl versus Sn–NCS bond on cytotoxicity is underway. The in vivo mammalian toxicity (LD_{50}, mg/kg) of compounds **6** and **7**, determined in Swiss albino mice by peroval route using the staircase method followed by pubit scale analysis[10] are found to be 630 and 960 respectively.

Table 1. ID_{50} values (μM) of dibenzyltin(IV) complexes against human cancer cell lines

Code[a]	MCF-7	WIDR	IGROV	MEL 19	A498	H226
1	11,000	11,000	150	11,000	11,000	11,000
2	19	63	63	29	19	25
3	1.3	10	0.9	4.6	2	7.4
4	2	14	1.8	6.6	3.3	3.3
4[b]	55.2	1000	502	100	67.5	1000
5[b]	57.7	100	150	100	75.5	>10,000
6	1.6	10	0.9	4.5	2	7.2
7	2.3	15	1.5	6.1	3	6.6
7[b]	59.1	100	450	1000	240	414
8[b]	61.5	1000	450	1000	414	1000
Cisplatin	467	450	75	260	400	1052
Carboplatin	2828	943	646	1481	4848	6734

[a]For compound code, refer to Table 1.
[b]Data from NCI-screening.

Under similar conditions, the LD_{50} values of carboplatin and cisplatin are found as 150 and 31, respectively. This result augments the fact that organotin compounds can reduce the toxic side effects generally associated with platinum drugs. The high cytotoxicity and reduced in vivo mammalian toxicity of the dibenzyltin(IV) complex make them potential candidate for further bioevaluation.

3-D QSAR Studies

Comparative molecular field analysis (CoMFA) studies has been used regularly to produce the three dimensional models which indicate the regions that effect the biological activity with a change in the chemical substitution. CoMFA method operates on a set of compounds superimposed to reflect their anticipated common bonding orientation.[11] CoMFA models describe the relative change in magnitude of the electrostatic and steric fields as a function of compound, sampled as function of spatial position around the compound set, and accounts for the variance in measured biological activity.

Data sets

In a total of 21 diorganotin complexes used for the CoMFA study, 14 complexes are selected from literature[8] (**L1**–**L14**, Scheme 2) and the remaining seven (**2**–**8**) from the present set (Scheme 1). In each analysis, the training sets constitute 18 complexes and the remaining three complexes are part of test sets (Table 2).

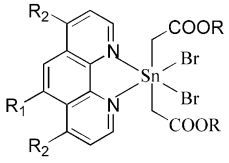

Code	R	R_1	R_2
L1	n-butyl	H	H
L2	Isobutyl	H	H
L3	n-pentyl	H	H
L4	Isopentyl	H	H
L5	1-methylbutyl	H	H
L6	n-butyl	NO_2	H
L7	isopentyl	NO_2	H
L8	1-methylbutyl	NO_2	H
L14	n-butyl	H	Phenyl

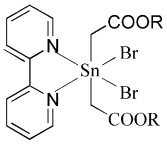

Code	R
L9	n-butyl
L10	Isobutyl
L11	n-pentyl
L12	Isopentyl
L13	1-methylbutyl

Scheme 2.

Structure generation

Complexes **L1** to **L8** and **L14** were generated from the X-ray structure of complex (4,7-*N*,*N*-diphenylphenanthroline)dibutyltindichloride.[12] Complexes **L9** to **L13** were generated from the X-ray structure of (2,2′-bipyridyl)diethyltindichloride.[13] The X-ray crystal structural analyses of the new dibenzyltin(IV) complexes **7** and **8** are carried out by us. Utilizing the latter, the structures of complexes **2**–**6** were generated. All structures were initially minimized in Sybyl with Gasteiger charges and further minimization was performed with MOPAC-6.0 using the PM3 method.[14,15] The optimized structures and MOPAC charges were considered for the further calculations. The octahedral geometry is maintained in all the structures.

Alignment

Two alignment rules were used for the superimposition of all complexes. In alignment-1, Sybyl database alignment method of 'AS_IS' was used along with highly active **3** as reference. A fragment containing Sn and two connected C-atoms (angle C–Sn–C $\sim$180°) was considered as a substructure for the alignment (Fig. 1). In alignment-2, Sybyl field fit was used to realign the molecules that were aligned with method alignment-1. The steric and electrostatic fields of **L1** to **L13** were fitted to the respective fields of **L14**. The fields of **2**, **4**–**8** were fitted to the fields of **3**. The molecular superimposition is nearly very similar in the both alignments.

CoMFA methods

CoMFA partial least square (PLS) analysis was performed using two different cytotoxic activities. The observed ID_{50} (μM) values were converted into $-\log(ID_{50})$ values and are reported in Table 2. All other default settings were used unless otherwise indicated. The steric and electrostatic fields were calculated using an sp^3 C-atom with +1 charge. The CoMFA grid spacing was considered as 2.0 Å within the defined region, which extended beyond the Van der Walls envelopes of the superimposed complexes at least 9.0 Å. For each cross-validated CoMFA analysis, the column filtering was set to 2.0 kcal/mol and set to 0.0 for the non-cross-validated analysis. The optimal number of components was designated such that cross-validated r^2 was highest and standard error of prediction was lowest.

CoMFA studies using MCF-7 activity

Complexes **L4**, **L9** and **6** constitute the test set, and the remaining as training set. CoMFA analyses were performed on both the aligned data sets. For alignment-1, r^2_{cv} of 0.874 and standard error of 0.646 is obtained, while alignment-2 produced r^2_{cv} of 0.833 and standard error of 0.663. Thus, alignment-1 with maximum r^2_{cv} was considered for the final PLS analysis, which yielded very good conventional r^2 with a very low error of estimate (Table 3). The ratio of steric and electrostatic field contributions is nearly 3:2. This CoMFA model was used to calculate the activity of three complexes in the test set. The actual and calculated activities of all complexes are given in Table 2. CoMFA steric (green and yellow) and electrostatic (red and blue) contours along with complex **7** are shown in Figure 2. The CoMFA model exhibited a very good ability not only to calculate the biological activity of training set complexes but also it is able to accurately predict the activity for the complexes in the test set.

Table 2. Actual and calculated antitumor activities ($-\log ID_{50}$) (μM) of complexes comprising of training and test sets of molecules

Code	MCF-7[a]		WiDr[b]	
	Actual	Calculated	Actual	Calculated
2	−1.28	−1.28	−1.80	−1.79
3	−0.11	−0.11	−1.00	−1.00
4	−0.30	−0.31	−1.15	−1.15
5	−1.76	−1.73	−2.00	−1.97
6	−0.20	−0.08	−0.99	−0.99
7	−0.36	−0.36	−1.18	−1.19
8	−1.79	−1.81	−3.00	−3.02
L1	−3.48	−3.39	−3.20	−3.15
L2	−3.31	−3.33	−3.16	−3.18
L3	−3.22	−3.33	−3.10	−3.12
L4	−3.54	−3.42	−3.18	−3.26
L5	−3.42	−3.41	−3.14	−3.17
L6	−3.25	−3.29	−3.13	−3.16
L7	−3.29	−3.29	−3.23	−3.22
L8	−3.29	−3.26	−3.20	−3.21
L9	−4.47	−4.42	−4.48	−4.43
L10	−4.34	−4.33	−4.39	−4.40
L11	−4.45	−4.38	−4.25	−4.26
L12	−4.45	−4.49	−4.45	−4.46
L13	−4.45	−4.47	−4.44	−4.20
L14	−2.46	−2.43	−2.59	−2.58

[a]Test set = **L4, L9, 6**; the rest are included in the training set.
[b]Test set = **L4, L13, 6**; the rest are included in the training set.

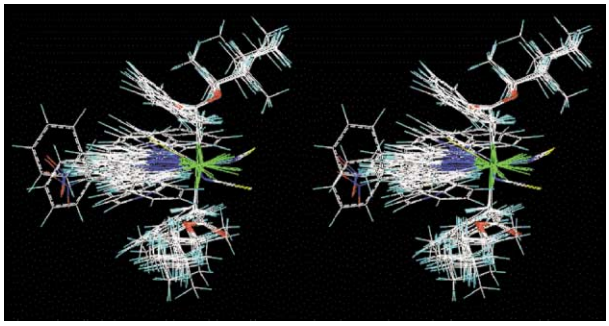

Figure 1. Stereoview of the superimposed complexes (training set) based on Alignment-1.

Table 3. Results of the CoMFA PLS analyses of the training sets

Parameters	MCF-7	WiDr
Cross-validated r^{2-} (r^2_{cv})	0.874	0.758
Standard error of predictions	0.646	0.683
Conventional r^2	0.999	1.000
Standard error of estimate	0.054	0.030
Number of components	6	6
F test values	2098	4022
Relative steric contributions	0.595	0.656
Relative electrostatic contribution	0.405	0.344

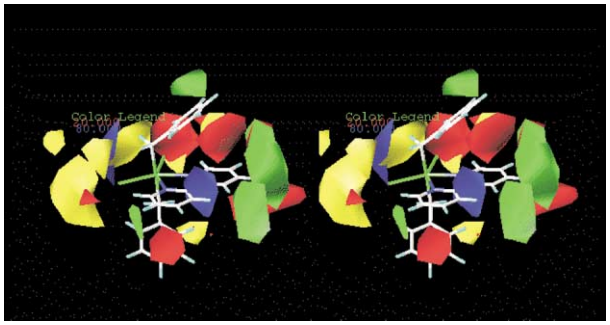

Figure 2. Stereoview of the CoMFA fields (MCF-7) along with complex **7**. The electrostatic fields are shown in red (negative) and blue (positive) polyhedra while the steric fields are shown in green (more bulky) and yellow (less bulky) polyhedra.

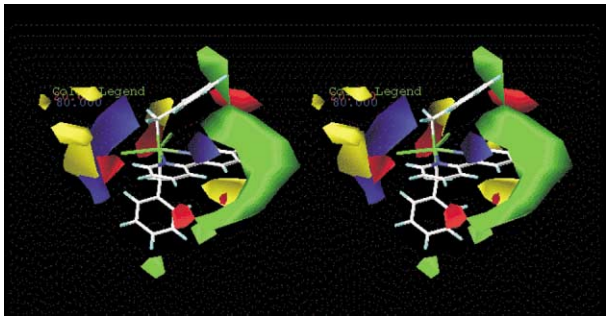

Figure 3. Stereoview of the CoMFA fields representing the WiDr biological activity. The nature of the fields is similar as in Figure 2.

CoMFA studies using WiDr activity

Complexes **L4**, **L13** and **6** constitute the test set while the remaining as training set. In the case of alignment-1, r^2_{cv} of 0.726 and standard error of 0.734 is obtained and in the case of alignment-2, these values are 0.758 and 0.683, respectively. Hence, PLS analysis was carried out using the alignment-2 as it is having higher r^2_{cv} and lower standard error. The PLS run without cross validation produced very good conventional r^2 and s (Table 3). Biological activities of test set complexes were predicted using the CoMFA fields, and compared with experimental data (Table 2). CoMFA steric and electrostatic contours are given in Figure 3. It is interesting to note that for both the cell lines, magnitudes of steric and electrostatics fields contributions are similar (Figs. 2, 3). This indicates perhaps a similar mode of action in the two cell-lines. It would be interesting to explore whether the hypothesis can be extended to other cell-lines also.

Structure–activity relationship

The outside region of bidentate ligand shows a greater flexibility for more bulky substitution (shown by green polyhedra in Figs. 2 and 3) compared to the similar region of Cl, Br or NCS substituents (shown by yellow polyhedra). This indicates the probable site of interaction. The stereoelectronic effect of alkyl groups on the interaction site is expected to be greater in a *trans–trans* dialkyl geometry as compared to *cis–cis* geometry. Even though they are in *trans–trans* geometry, the dibenzyl groups are significantly away from the interaction site, by virtue of the π–π stacking interaction of the benzyl aromatic ring with the ligand aromatic residue. The observed higher cytotoxic activities of the dibenzyltin complexes as compared to other dialkyl derivatives might well arise from such a phenomenon. The little red polyhedra along the Sn–Cl or Sn–NCS bonds indicate the higher activity for the groups with more negative charge and it is consistent with the general observation that Cl-substituted complexes are more active than either Br- or NCS-analogues. Any other groups which are less sterically bulky, and more negative will have a positive effect on the biological activity.

References and Notes

1. (a) Rosenberg, B.; VanCamp, L.; Trosco, J. E.; Mansour, V. H. *Nature* **1969**, *222*, 385. (b) *Metal Complexes in Cancer Chemotherapy*; Keppler, B. K., Ed.; VCH: Weinhein, 1993.
2. Gielen, M. *Coord. Chem. Rev.* **1996**, *151*, 41.
3. (a) Casas, J. S.; Castineiras, A.; Rodriguez-Arguelles, M. C.; Sanchez, A.; Sordo, J.; Vazquez Lopez, A.; Pinelli, S.; Lunghi, P.; Ciancianaini, P.; Bonati, A.; Dall'Aglio, P.; Albertini, R. *J. Inorg. Biochem.* **1999**, *76*, 277. (b) Cagnoli, M.; Alama, A.; Barbieri, F.; Novelli, F.; Bruzzo, C.; Sparatore, F. *Anticancer Drugs* **1998**, *9*, 603. (c) al-Allaf, T. A.; Khuzaie, R. F.; Rashan, L. J.; Halaseh, W. F. *Boll. Chim. Farm.* **1999**, *138*, 267. (d) Gielen, M.; Dalil, H.; Mahieu, B.; Biesemans, M.; Willem, R. *Appl. Organomet. Chem.* **1998**, *12*, 855. (e) Gielen, M.; Dalil, H.; Biesemans, M.; Mahieu, B.; de Vos, D.; Willem, R. *Appl. Organomet. Chem.* **1999**, *13*, 515.
4. Li, Q.; Yang, P.; Wang, H.; Guo, M. *J. Inorg. Biochem.* **1996**, *64*, 181.
5. (a) Crowe, A. J.; Smith, P. J.; Atassi, G. *Chem. Biol. Interact.* **1980**, *32*, 171. (b) Jiazhu, W.; Hunag, J. *Inorg. Chim. Acta* **1988**, *152*, 67. (c) Shenazhi, H.; Dashuang, S.; Wan, H. T. *Inorg. Chim. Acta* **1990**, *173*, 1. (d) Crowe, A. J.; Smith, P. J.; Atassi *Inorg. Chim. Acta* **1984**, *93*, 179. (e) Biddle, B. N.; Johns, G. *Appl. Organomet. Chem.* **1989**, *3*, 537. (f) Zhenaauan, Z.; Huad, P. *Appl. Organomet. Chem.* **1991**, *5*, 183.
6. Crowe, A. J.; Smith, P. J.; Cardin, C. J.; Parge, H. E.; Smith, F. E. *Cancer Lett.* **1984**, *24*, 45.
7. (a) Samuel, P. M.; Roy, S.; Jaiswal, K. A.; Rao, J. V. *J. Appl. Toxicol.* **1998**, *18*, 383. (b) Sinha, P.; Kundu, A.; Roy, S.; Prabhakar, S.; Vairamani, M.; Ravi Shakar, A.; Kunwar, A. C. *Organometallics* **2001**, *20*, 157 and references therein.
8. Gielen, M.; de Vos, D.; Pan, H.; Willem, R. *Main Group Metal Chem.* **1992**, *15*, 243.
9. (a) Boyd, M. R. *Principles and Practice of Oncology* **1989**, *3*, 1. (b) Enna, S. J.; Synder, S. H. *Mol. Pharmacol.* **1977**, *13*, 442.
10. Ghosh, M. N. *Fundamentals of Experimental Pharmacology*; Scientific Book Agency: India. 1971.
11. Cramer, R. D., Jr.; Patterson, D. E.; Bunce, J. D. *J. Am. Chem. Soc.* **1988**, *110*, 5959.
12. Sheng-zhi, H.; Wenfeng, L.; Jiazhu, W.; Zexing, H. *Jiegou Huaxue (J. Struct. Chem.)* **1989**, *8*, 36.
13. Chadha, S. L.; Harrison, P. G.; Molloy, K. C. *J. Organomet. Chem.* **1980**, *202*, 247.
14. SYBYL 6.5 *Molecular Modeling Software*, Tripos Associates Inc., 1699 S. Hanley Road, St. Louis, MO 63144-2913, USA.
15. (a) Stewart, J. J. P. *J. Comput.-Aided Mol. Des.* **1990**, *4*, 1. (b) MPOAC Version 6.0, QCPE 688, Bloomington USA, 1995.